

## Slope failure in stratified rocks: a case from NE Himalaya, India

**Abstract** Mountainous regions of India experience recurrent slope failures due to rapid urbanization. The main causes of slope failure are high precipitation aided by unplanned construction of cut slopes. Such slope failures are further aggravated because of the presence of low strength, highly jointed, stratified rocks rich in clay minerals. In general, effect of weathering is more pronounced in these rocks, which causes long-term time-dependent deterioration of the rocks as well as joint strength. In this regard, the present investigation deals with the causes, behavior, and mechanism of slope failure by examining a section in the North Eastern Himalayas. A detailed field investigation was carried out for examining the existing condition of slope, slope material, and joint parameters. Laboratory experiments like compressive and tensile strength tests along and across the lamination planes along with slake durability index tests were conducted to characterize the material and investigate the role of weathering in strength degradation. Later, numerical simulation was performed employing distinct element method to investigate the failure behavior, mechanism, and also the effect of water pressure in destabilizing the slope. The experimental result indicates directional strength variations parallel and perpendicular to bedding plane, which makes the rock incompetent to sustain external load. The presence of orthogonal joint sets accelerates the process of block detachment. Significant slaking was observed which further deteriorates and fragments the rock at deeper level. Numerical simulation shows that failure plane is dominantly planar (along the bedding parallel joints) and surficial.

**Keywords** Shale · Stratified rocks · Rock joints · Cut slope failure · Weathering · Distinct element method

### Introduction

A cut slope failure was triggered on May 11, 2013, in Chaltlang, Aizwal, India. The outcome of the disaster was very severe causing death of around 35 people, damaging several houses and disruption of socioeconomic activities and transportation lines. The slope failure was triggered by incessant rainfall for the past couple of days (Ghosh and Chakchhuak 2013; Singh et al. 2016b). The cut slope material constitutes stratified structure of siltstone-sandstone shale with a pronounced bedding plane dipping toward the slope face. Such outcrops are very common in the northern reaches of the Himalayas and probably at many other places along the transportation corridors. In such scenarios, slope failure along transportation lines face severe threat of landslide hazards and has been a problem in hilly areas around the world (Evans and Hungr 1993; Regmi et al. 2013; Singh et al. 2016c).

Stratified sedimentary rocks are often encountered in both natural and man-made slopes (Stead 2016). Stability problems are always associated with stratified rock mass mostly due to human infringement. The dip and mechanical properties of bedding plane bear significant effect on the strength and stability of stratified rocks and planar failure is the most common cause of rockslide (Tang et al.

2016). Stratified rocks are distinguished by the characteristic bedding planes and alternate layering of rocks of variable thickness. Strength anisotropy is one of the most distinct feature of stratified rocks which can affect hydraulic, mechanical, thermal, and even seismic behavior of rocks (Khanlari et al. 2015). Anisotropic strength behavior has been studied by several researchers, and a preliminary investigation indicate that the rock possess least strength when weak planes are inclined at 30°–45° to the applied load (Donath 1961; Nasser et al. 2003; Khanlari et al. 2015; Martin et al. 2016). They are known to be highly notorious material because of wide variation in engineering properties and intense modification from the geomorphic agents (Stead 2016). Therefore, several casualties often occur in stratified rocks where improper design of civil structures has led to the failure of the slope material.

Bedding planes are the weakest zone in stratified rocks and are highly persistent unless dissected by other joints. Einstein et al. (1983) have studied the effect of persistence of joints on rock slope and suggested that a small variation in persistence may produce large variation in resistance offered by the slopes. In such jointed rocks, layer parallel slip usually occurs, which may resemble a typical planar failure with a condition that joints must be shallower than the slope face. In stratified and jointed rocks, sliding is almost always accompanied by internal deformation leading to the distribution of nonuniform shear stress along the discontinuity plane causing the initiation of progressive failure (Gencer 1985). However, Eberhardt et al. (2004) explains that where suitably oriented discontinuities are highly persistent, failure mechanism requires very little damage for kinematic release. Progressive failure in such rock mass is regulated by the development of continuous sliding surface and reduction in shear strength from peak to residual values (Bjerrum 1967).

It has been observed that surface degradation and landslides generally occur in slopes excavated in soft rocks and deterioration of surface as well as subsurface rocks starts relatively shortly after the excavation (Mišćević and Vlastelica 2014). The properties and behavior of exposed clay-rich rocks along cut slope to external influences are dominantly controlled by the mineralogical composition, preconsolidation history, composition of cementing material, and texture and level of cementation (Števančić and Mišćević 2007). In such clay-rich rocks, water plays greater role in modifying their physical properties and decomposition of binding material which leads to disintegration of rock into smaller fragments. Moreover, shales have low effective porosity which confines fluid to flow only through the fractures. Several authors have performed experimental study on fluid flow through single fracture under different stress environment and observed that a linear relationship exists between discharge ( $Q$ ) and fluid pressure ( $f_p$ ), and  $Q$  is significantly less for large sample as compared to small sample (Singh et al. 2015a, 2016a). This effect becomes negligible at higher confining stresses, i.e., >10–15 MPa. However, rocks along the cut slopes generally have very low confining stress, and as a result, a large fracture opening is expected due to high  $f_p$ .

Appraisal of stability problems becomes very difficult in stratified rocks because of strength anisotropy, high rate of weathering, wide variation in engineering properties, and failure mechanism. This is an active field of research in rock engineering and has been attempted by many researchers by employing numerical and experimental methods. Numerical method is an essential tool for assessing any stability problems associated with rock engineering because of its capability to solve complex problems. Many authors have used the conventional limit equilibrium method (Tang et al. 2016) owing to its simplicity; however, others have also used advanced methods like finite and distinct element methods (Eberhardt et al. 2004; Kainthola et al. 2012; Singh et al. 2015b; Mahanta et al. 2016). The failure problems associated with stratified slopes clearly belong to the domain of discontinuum method, and Universal Distinct Element Code (UDEC) is believed to be highly capable and widely accepted among rock engineers to solve complex problems (Cundall and Hart 1992; Jing and Hudson 2002; Bobet et al. 2009; Kainthola et al. 2015). The present study uses above-mentioned information from past stratified cut slope failure to investigate the stability of hill slope of Chaltlang, Mizoram, India (Fig. 1). A detailed experimental investigation was done to characterize the anisotropic strength of rocks and understand

their behavior due to long-term weathering. Additionally, stability analysis was done employing distinct element method (DEM) to examine the process and mechanisms responsible for failure in stratified rocks under mechanical and coupled hydromechanical loading.

#### Lithology and structures

Lithologically, Surma group of rocks mainly occupy the core of the anticlines and are the major lithounits exposed in the state of Mizoram. It is mainly represented by Bokabil and Bhuban Formation (Fig. 2). Bhuban Formation is further subdivided into lower, middle, and upper formations based on lithological and physical characters as well as the order of superposition. Lower Bhuban Formation is predominantly arenaceous and composed of fine to very fine grained, compact, thickly bedded lithic greywacke along with massive but less compact sandstone. The shales are dark gray, micaceous, and splintery in nature. Middle Bhuban Formation conformably overlies Lower Bhuban Formation with gradational contact. This formation is mostly argillaceous and characterized by thinly bedded shale, siltstone, and sandstones. Shales in this formation are splintery too and moderately hard, but sandstones are comparatively soft and friable. Upper Bhuban Formation also

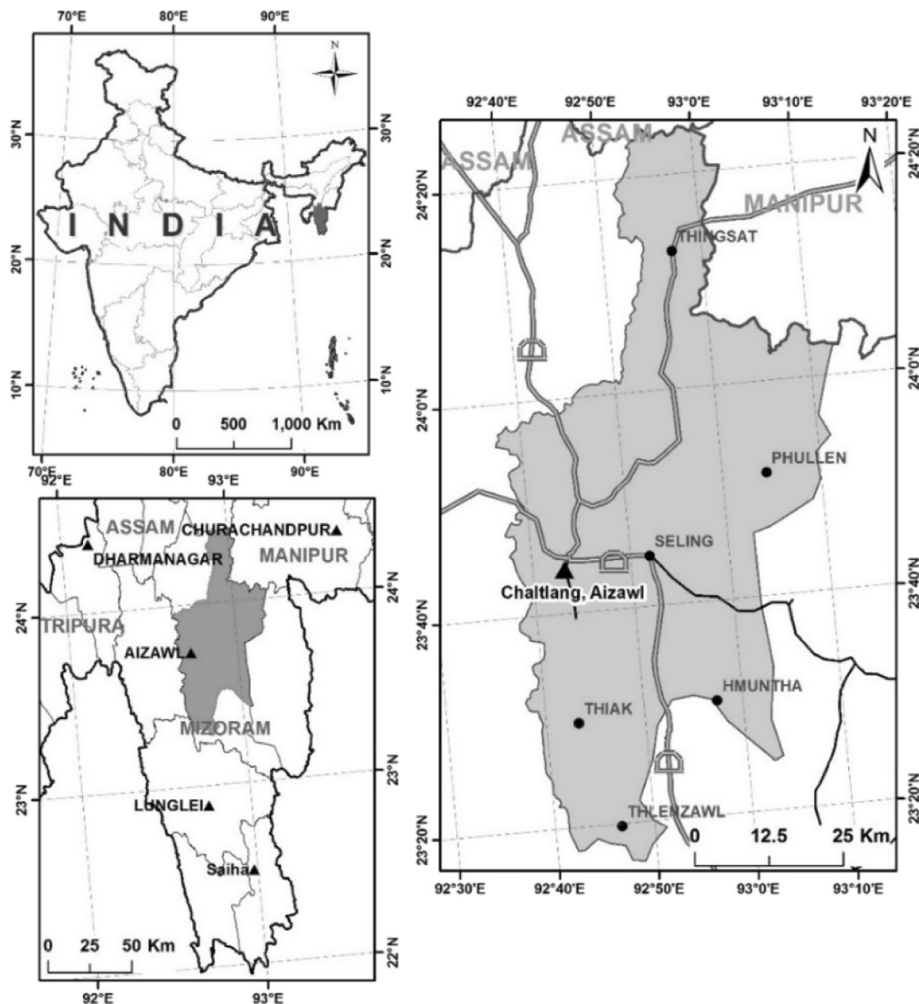
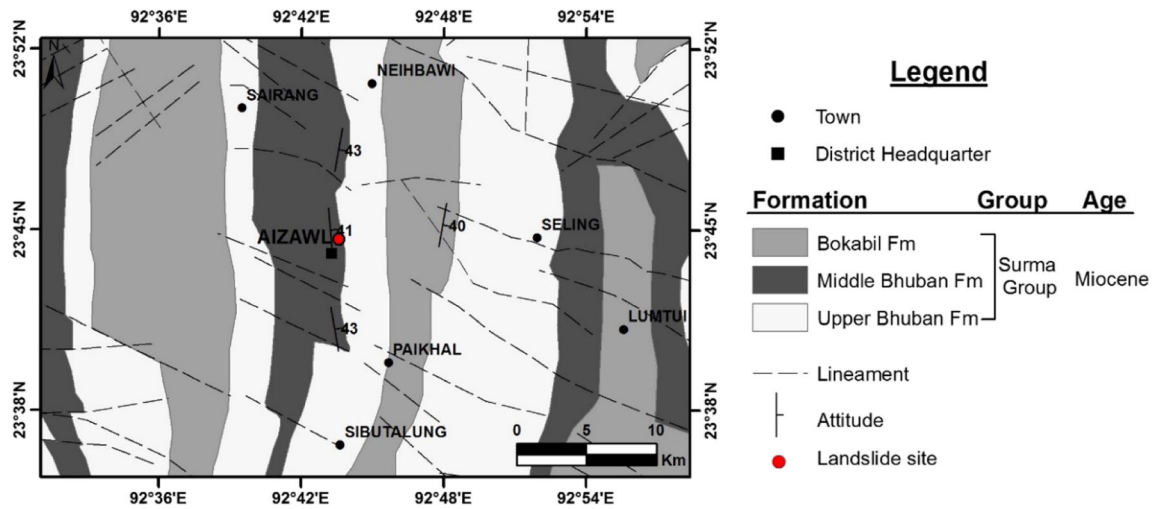


Fig. 1 Location of failed site in the study area



**Fig. 2** Lithology map of the study area showing different structural elements (modified after Prasad 1983, unpublished)

conformably overlies the Middle Bhuban Formation showing gradational contact. The formation is mostly arenaceous mainly represented by thick sandstones. Unlike previous sandstones, these are relatively hard and compact. Occasional occurrence of thinly bedded micaceous sandstones with subordinate siltstones and shale also occurs within this unit. However, shales in this section are also splintery and break into fragments due to cross jointing. Apart from these rocks, shelly limestone, calcareous sandstone bands, and pebble beds are also present in this formation. Bokabil Formation also showing gradation contact overlies the Upper Bhuban Formation. It is mostly argillaceous comprising mainly of shale, siltstone, and thinly bedded sandstones and occurs on the flanks of anticlinal ridge or in the cores of synclines.

The major structural trends in the region coincide with the regional tectonic trends. The average strike of the bedding varies from NNE-SSW with dips varying from 40° to 50° either toward east or west. The sediments are folded into tight symmetrical synclines and anticlines along N-S axis. Siltstones and shale units have mostly developed macroscopic folds in comparison to sandstone units. Faults observed in this area are of transverse, longitudinal and oblique types affecting the folded sequence although the majority are longitudinal strike faults.

## Methodology

### Field investigation

Aizawl District is the largest city (area of 4.57 km<sup>2</sup>) in the state of Mizoram and is densely inhabited with a population of about 300,000. The entire city is situated on a ridge with rugged topography of height 1132 m above mean sea level (msl). Geological survey was carried out in and around Chaltlang, Mizoram, India, to investigate the cut-slope failure. During field investigation, it was observed that the hill slopes are very steep and a number of multistoried buildings were constructed in an unplanned manner (Fig. 3a, b). The rocks exposed in the studied cut slope section are moderately to highly weathered silty shale, sandstone, and siltstone. Clay material is present within the joints, probably derived from chemical weathering of in situ rocks. Lithological and structural details were collected from the affected area and the exposed

rocks in the surrounding. Weathered, variegated color, thinly bedded siltstone and shale were observed near the cut-slope failure site. The elevation of the toe and crest is 1110 and 1160 msl, respectively. Three sets of joints are present viz., Bedding plane, J<sub>1</sub> (N5° W/45° E), J<sub>2</sub> (N85° E/90°), and J<sub>3</sub> (N10° E/70° SE). The general trend of the slope face is 10° NW, dipping toward 55° NE. About 10 to 15 numbers of houses were affected due to this slope failure. It was observed that the drainage from the houses were flowing over the slope and no proper drainage channels were present. Figure 3a, b shows photographs of the investigated area before and after slope failure, respectively. Figure 3c, d shows failed cut slope and destroyed buildings below the road as well as on the slope face.

### Material characterization

Material characterization is an integral part of engineering geology. It gives an idea about the health of rocks and its ability to sustain engineering load. In stratified rocks, problem arises due to the presence of weak planes (lamination, bedding planes, schistosity, cleavage, and discontinuities) which makes them a complex material to study and determine reliable engineering properties. Therefore, it becomes imperative to investigate the physical and geomechanical properties of these anisotropic rocks in relation to loading direction. For this purpose, several rock blocks of approximate dimension 0.12 × 0.08 × 0.14 m<sup>3</sup> were collected from the freshly exposed slope surface along with smaller blocks from the dislodged material. The different geomechanical properties viz., density, natural moisture content (NMC), strength (UCS and tensile strength), shear strength (cohesion, C, and internal angle of friction, φ), elastic modulus, and Poisson's ratio, were obtained experimentally in laboratory.

Deformation in laminated rocks is mostly controlled by the loading direction in relation to the plane of lamination and confinement state (Fig. 4). Although there can be several cases (0°–90°) depending on the inclination of lamination, the most critical are the ones which are either parallel or inclined at some angle. To investigate strength anisotropy in the present study, samples were prepared in four different orientations of weak planes (0°, 30°, 45°, and 90°) to the applied load (Fig. 4). The diameter (D) of the

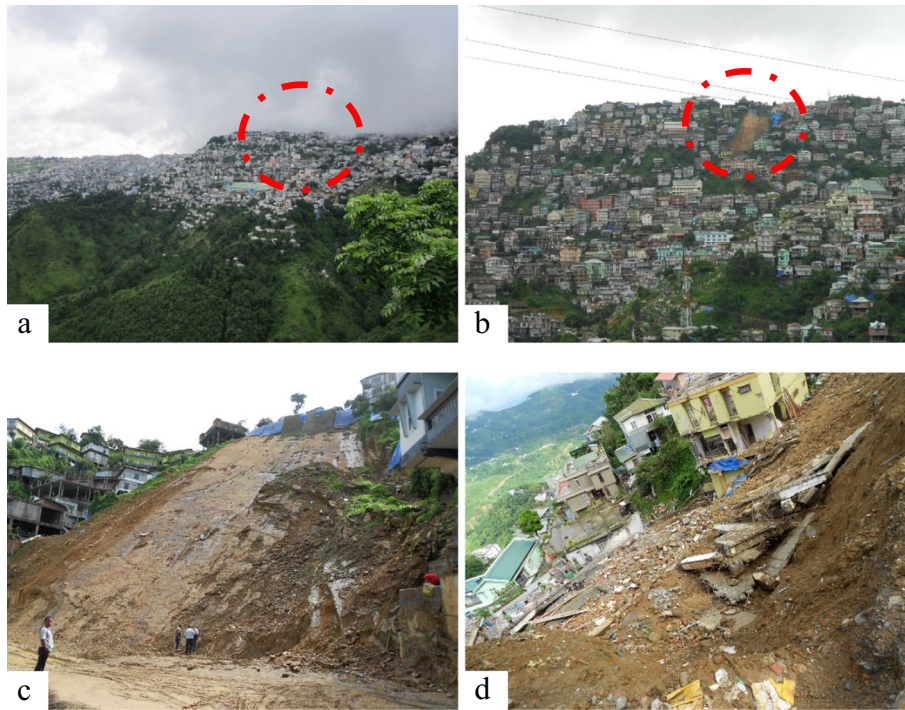


**Fig. 3** Field photographs showing a dense urbanization, stable slope before failure, b post-failure condition, c failed cut slope section, and d collapsed buildings due to slope failure

drilled cores was maintained at 0.054 m with a length to diameter ratio of 2:1 (ASTM-D4543 2008). A total of 12 core samples for UCS (average of three samples for four cases) and five for BTS were prepared to study the influence of planar anisotropy on the strength of rocks. Strength anisotropy in rocks like mudstones, siltstones, and schist have been studied by several researchers in the past (Donath 1961; Yaşar 2001; Nasseri et al. 2003; Khanlari et al. 2015; Martin et al. 2016). The review of their work suggests

that the maximum and minimum strength occurs at around  $90^\circ$  and  $30^\circ$ , respectively, to the direction of loading. This is true for both confined and unconfined conditions. The only change which affects the samples in confined state is increase in load-bearing capacity, which is obvious. Similar data have also been collected for three different laminated rock types from previous studies to compare the present results and understand the strength anisotropy in relation to different laminated rock types. The result of

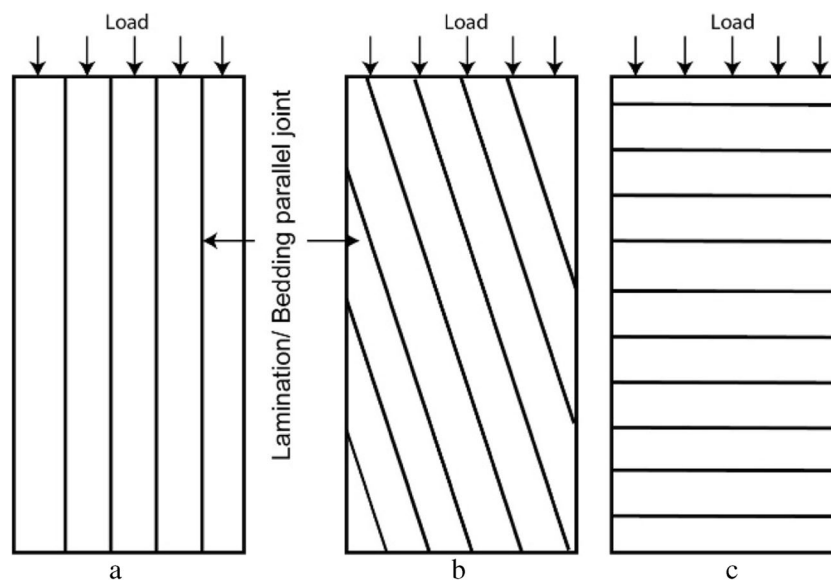


**Fig. 4** Loading in different direction to the plane of lamination (test performed at  $0^\circ$ ,  $30^\circ$ ,  $45^\circ$ , and  $90^\circ$ )

UCS and BTS along with other properties is presented in Table 1, and a comparative analysis of strength anisotropy in stratified rocks is discussed in later section.

Under uniaxial loading, fractures are free to grow without any resistance from other directions. Primary cracks (tensile) grow in a stable manner and appear first, while secondary cracks (shear cracks) appear at a later stage of loading and, in most cases, lead to the failure of specimen. The propagation of shear cracks has been a matter of argument among researchers; however, most experimental results have shown them to propagate in the plane of preexisting cracks (Bobet and Einstein 1998). This has led to a notion that the propagation of secondary cracks may be material-dependent. The process of crack coalescence and propagation becomes highly complex in a multiple crack system. In this regard, Wong and Einstein (2009) experimentally studied cracking and coalescence behavior of molded gypsum and Carrara marble containing two preexisting parallel cracks. Based on coalescence types, they were able to identify nine different categories characterized by crack types and that the material does have the effect on initiation and propagation of cracks. Eberhardt et al. (1998) points that failure under uniaxial compression is a result of coalescence of numerous micro cracks which grow in the direction of major principal stress ( $\sigma_1$ ). If the cracks are not suitably oriented (i.e., aligned with  $\sigma_1$ ), they tend to grow along curve paths to align themselves with  $\sigma_1$  (Fig. 5).

Failure behavior and strength is significantly affected by the presence of planar anisotropy (bedding, schistosity, cleavage). Donath (1961) performed a series of test on anisotropic rocks (slate and shale) and suggested that at low confining pressures, inclination of planar anisotropy has significant effect both on breaking strength as well as on the angle of developed shear fracture. Shear fractures developed parallel to the bedding planes until 45° in slate (confinement of 3.5 MPa); however, anisotropy had insignificant effect on shale samples after 30° for a confinement of 42 MPa. This simply means that at a greater depth (large overburden), the effect of anisotropy on shear fracture will be negligible due to high confining stresses and fractures will tend to develop nearly parallel to the loading direction.

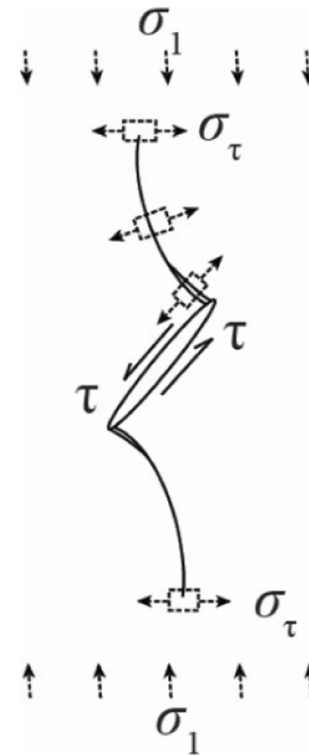


**Fig. 5** Crack initiation and propagation from the tip of micro-crack parallel to  $\sigma_1$  (after Eberhardt et al. 1998)

In the present study, planar anisotropy showed pronounced effect on the strength as well as the failure mode of the silty shale samples under uniaxial loading. For laminations inclined at 30°, failure occurred by sliding along weak planes but mixed failure mode was observed for other cases. Typical tensile splitting was observed in sample loaded perpendicular to the lamination along with secondary failures parallel to the laminations. Singh et al. (2016d) argues that axial splitting is common in samples without predefined weak planes; however, a combination of shear and

**Table 1** Some properties determined in laboratory to characterize the slope material

Sl. no.	Parameters	Miz 1	Miz 2	Miz 3	Mean	Std. dev.
1	Density ( $\text{kg/m}^3$ )	2279.00	2307.00	2314.00	2300.00	15.12
2	NMC (%)	6.30	6.12	6.15	6.19	0.08
3	UCS (0°)	17.43	13.95	18.74	16.71	2.02
	UCS (30°)	9.85	6.78	8.89	8.51	1.28
	UCS (45°)	13.58	11.29	10.38	11.75	1.35
	UCS (90°)	27.92	34.48	35.4	32.60	3.33
4	BTS (MPa)	3.52	2.61	1.23	2.45	0.95
5	C (MPa)			8		
6	Phi (°)			34		
7	E (MPa)			11,000		
8	$\nu$			0.29		

tensile failure modes is observed almost in all samples. Chen et al. (1998) also observed tensile splitting as the dominant mode of failure when inclination of layers vary from  $0^\circ$  to  $60^\circ$  or at  $90^\circ$ ; however, shear failure along the layers with and without branching was dominant in the range of  $60^\circ$  and  $90^\circ$ . Khanlari et al. (2015) showed that anisotropic strength and failure pattern of laminated sandstone depend to a large extent on the angle between lamination plane and loading direction and least strength was observed at an inclination of  $15^\circ$ – $30^\circ$  in the case of both compression and tension mode. Gao et al. (2015) have studied the mechanical behavior of anisotropic shale and observed that the strength of shale in compression is much higher than that of tensile and even failure patterns are very complex. In addition, the tensile strength parallel to the bedding planes is about 300 times that of normal to bedding layer. This relative contrast in strength anisotropy observed in laminated rocks contributes to the development of kinematic release, particularly in situations where orthogonal joints are widely spaced (Stead 2016). Kinematic analysis was done using lower hemisphere equal area projection with three joint sets. The laminations are near parallel and daylight on the slope face along with two other joints, one almost perpendicular to the slope face (Fig. 6).

Slake durability test was performed on the samples collected from the exposed surface as well as the failed mass to investigate the durability of weak rocks. An obvious drop in durability index was observed after the second cycle in both the cases. However, major disintegration was observed in the latter case (Table 2). Bell et al. (1986) suggests that in the case of mudstones, slaking behavior is dominated by tendency to break along irregular fracture planes but when well-developed may cause disintegration well within one to two cycles of wetting and drying. While swelling disrupts the structural integrity of shale mass, shrinkage allows development of fractures along existing micro cracks leading to decrease in shear strength and simultaneous increase in hydraulic conductivity (Yagiz 2001).

Shales have very high total porosity but extremely low effective porosity and permeability. This distinct property allows water to retain into the pores and allows development of considerable pore water pressure. Therefore, groundwater/seepage due to heavy

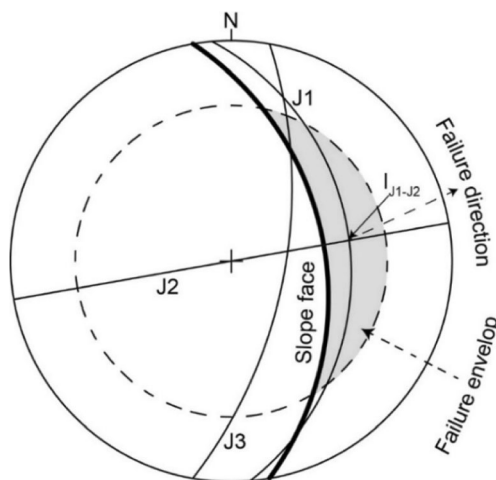


**Fig. 6** Lower hemisphere equal area projection showing kinematic stability of blocks

precipitation is also among the major causes of slope failure in clay-rich rocks. In addition, presence of clays and adverse climatic conditions intensifies the rate of weathering. Considerable strength reduction due to dissolution of cement and even change in failure behavior is also observed with continued weathering of clay-rich material. Slaking nature of such material allows water to ingress much deeper causing fragmentation. Therefore, construction in clay bearing rocks is one of the major challenges because of their susceptibility to degrade and weather rapidly upon exposure (Gökçeoglu et al. 2000).

### Numerical simulation

Clay-rich rocks are high in porosity but generally impermeable. Therefore, fluid flow is mainly governed through fracture networks. It is to be noted that permeability of jointed rock is several orders of magnitude greater than intact rock (Brace 1978). In addition, rocks such as shale have high porosity but are incapable to transmit fluid through matrix due poor interconnectivity between the grains. Therefore, in condition of heavy precipitation, a common understanding suggests that the stability of weak and jointed rock slopes will be affected by the level of water behind it and transmission of fluid will be through the weak planes like laminations/joints or interface between the strata. In order to understand the behavior of laminated rocks under gravity and coupled hydromechanical conditions, distinct element method (DEM) is mostly preferred. A system comprising of an interface between the discrete blocks is considered a discontinuum and can be effectively modeled in universal distinct element code (UDEC) with the benefit of finite displacement and rotation of discrete bodies including complete detachment (Cundall and Hart 1992). UDEC allows discretization of domain into blocks using a finite number of discontinuities. The block is further subdivided for calculation of stress, strain, and displacement (Bobet et al. 2009; Lisjak and Grasselli 2014). The purpose of selecting UDEC is obvious because of its ability to model large strain, interface behavior and to study of response of slope under coupled hydro-mechanical simulation.

### Mechanism of fluid flow in joints

Fluid flow is performed in a fully coupled hydromechanical analysis meaning that conductivity through fractures will be affected by mechanical deformation; conversely, fluid pressure will also affect the behavior of fractures (Jing et al. 2001). Fluid flow in UDEC makes use of domain structure assumed to be filled with fluid at uniform pressure at constant pressure. Each domain in the network is separated by contact points at which the mechanical interaction between the blocks is established (Indraratna et al. 1999). In each domain, uniform fluid pressure exists in the absence of gravity, whereas the pressure varies linearly following hydraulic gradient in problems with gravity. Depending upon the

**Table 2** Slake durability index of studied samples

Samples	SDT after first cycle (%)	SDT after second cycle (%)
Fresh exposed surface	86	79
Failed mass	75	54

configuration of contact (Point or edge), flow rate can be calculated in two different ways (Eqs. 1 and 2).

$$q = -k_c \Delta p \quad (1)$$

where  $k_c$  is the point contact permeability factor, and

$$\Delta p = p_2 - p_1 + \rho_w g (y_2 - y_1) \quad (2)$$

where  $\rho_w$  is the fluid density,  $g$  is the acceleration due to gravity, and  $y_1$  and  $y_2$  are the coordinates of domain centers.

In the case of planar fractures with edge to edge contact, cubic law for parallel plate model (Witherspoon et al. 1980) can be assumed for estimating the flow rate, given by Eq. 3.

$$q = -k_j a^3 \frac{\Delta p}{l} \quad (3)$$

where  $q$  is the flow rate,  $m^3/s$ ,  $k_j$  is the joint permeability factor,  $Pa^{-1} s^{-1} (1/12 \mu)$ ,  $\mu$  is the dynamic viscosity of the fluid,  $Pa s^{-1}$ ,  $a$  is the contact hydraulic aperture, m, and  $l$  is the length assigned to the contact between the domains, m.

#### Geological profile and problem formulation

Total station survey was used to obtain the coordinates and other data points. These point data were later used for further processing in AutoCad software to obtain the topographic map. The desired profile section was obtained directly from the topographic map. Over this geological section, an assumed initial topography was superposed to highlight the conditions before failure. There are number of houses on the top of the slope which remained undisturbed while few others over the slope face were completely damaged due to failure. The assumed section which represents the initial topography was used to model the slope face to achieve the present condition. The height of the modeled slope is 50 m from the mean sea level of 1100 m. The present slope angle is  $45^\circ$  with planar to curvilinear surface, while the assumed topography represents a slope angle of around  $50^\circ$ . The upper slope material constitutes of silty shale with alternate layering of siltstone, sandstone, and shale (Fig. 7). The geometry includes two joint sets in

which laminations are assumed to be infinitely long and modeled as persistent set, while the orthogonal tectonic joints are modeled as impersistent set.

Initially, gravity loading is done to bring the system to equilibrium followed by addition of water head of 40 m on the left boundary of the slope. This value of fluid pressure was applied keeping in mind the incessant rainfall since last few days. Joint properties were reduced in the second phase to accommodate the loss in shear strength due to continuous sliding in addition to decomposition and degradation of interface material by accumulation of water. The movement of bottom as well as left boundary is restrained in both X and Y direction, while bottom boundary is made impermeable to maintain fluid pressure. The joint properties used in the model are partly determined in laboratory and partly through Itasca's user guide (Table 3).

#### Results and discussion

The low value of UCS for both exposed and failed mass is an indication to the continued effect of weathering. Moreover, a sharp decrease in the strength of the samples loaded in perpendicular and parallel to lamination is another factor that decreases the load-bearing capacity and promotes kinematic release of blocks. A better understanding of strength anisotropy is made from Fig. 8, where UCS and angle of lamination are plotted on ordinate and abscissa, respectively. The graph compares the result of four different laminated rocks including one from present study. The trend of all the rocks is almost similar with the minimum strength value somewhere around  $30^\circ$ – $45^\circ$ . Silty shale samples from present study follow the trend of Opalinus clay samples tested by Martin et al. (2016). Laminated siltstone samples tested by Yaşar (2001) show highest strength followed by biotite schist samples (Nasseri et al. 2003). It is interesting to correlate the findings from Fig. 8 with the stratification observed in the cut slope face in the present study. The bedding parallel joint dips toward slope face with an amount of  $45^\circ$  which indicates that the rock mass is likely to show least strength when the slope is loaded from the top. This important parameter is generally ignored while construction of houses which ultimately leads to failure of cut slope.

Mudstones when dry possess relatively high strength in comparison to significantly lower values observed in saturated

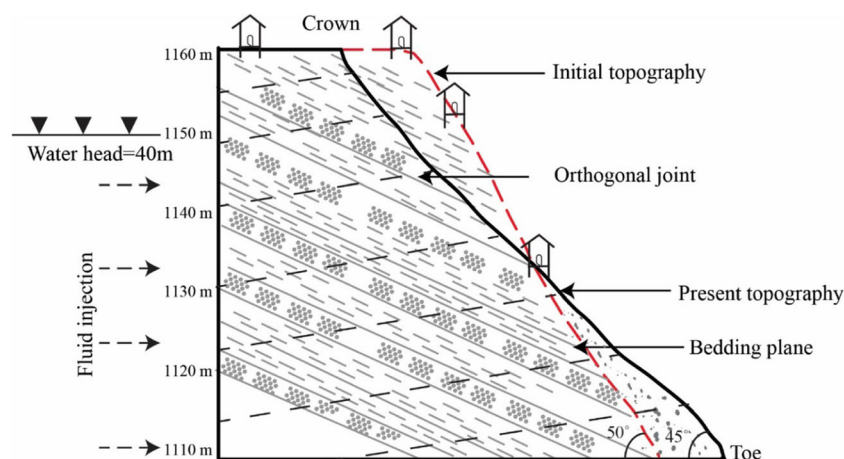


Fig. 7 Schematic diagram showing condition of slope prefailure and modified topography

**Table 3** Joint properties used in the numerical simulation

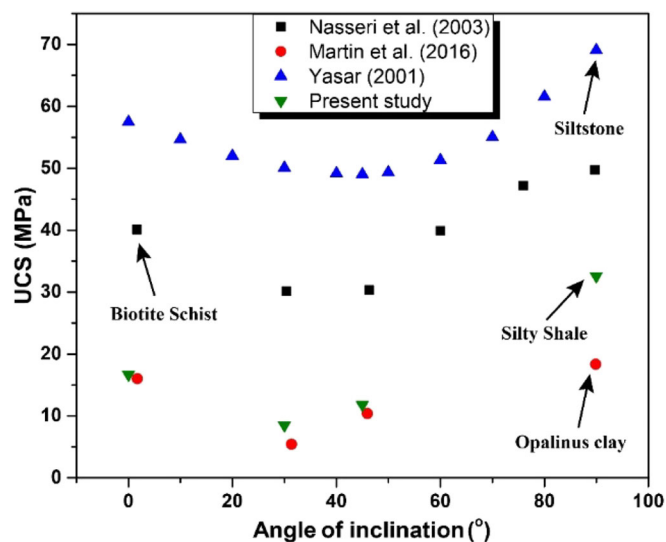
Parameters	jcohesion (MPa)	jfriction (°)	jperm (MPa <sup>-1</sup> s <sup>-1</sup> )	ares (m)	azero (m)
Gravity	0.05	25	1E8	1E-4	1E-4
Coupled	0.005	20	1E8	2E-4	5E-4

conditions. This happens due to the basic reason that water breaks the diagenetic bonds between the mudstone grains and destroys their integrity to cope with engineering loads (Lee et al. 2007). The slake durability index of the analyzed samples confirms the same as samples show significant disintegration after the second cycle. In slopes where interbedded shale and sandstone are present, water is retained in the interface between the highly permeable sandstones and less permeable shale making the interface highly susceptible to failure (Lee et al. 2007). Shale has a potential to absorb sufficiently large volume of water as a result of which failure is often accompanied by reduction in shear strength (Yagiz 2001).

The failure mode observed from kinematic analysis in the studied cut slope suggests planar type dominating over other modes. The widely spaced orthogonal joint sets allow water to percolate in the near vertical available joint spaces leading to the development of pore pressure perpendicular to joint walls enabling kinematic release of the blocks (Fig. 9). A number of failure modes have been reported in laminated rocks particularly in shales, mudstones formations right from translational, toppling, rockfall, and even earthflows (Bovis 1985; Geertsema and Cruden 2009; Goodman 2013). However, flow-like movement has been reported to be the most widespread than other types by Urciuoli (1990) while studying landslides in highly fissured tectonized clay shales. Picarelli et al. (2006) further suggest that outcrops in such material are generally overlain by a veneer of soft and nonfissured clay produced by weathering and swelling which is consistent with the field observation (Fig. 9).

To further investigate the mechanism of failure, numerical simulation was performed using distinct element method. The

numerical study was studied in two phases. Initially, the slope was brought to equilibrium by gravity loading with a maximum displacement of around 0.07 m near the crest of slope (Fig. 10). The equilibrium state in the numerical model is a condition which is achieved when the unbalanced force tends to zero. This is shown by force vs time graph where unbalanced force on ordinate axis keeps on decreasing until the model has achieved equilibrium (Fig. 10 subset). Stress concentration and disturbance can be seen near the slope face, but the shear strength of the interface is just not enough to cause or initiate any sliding. However, time-dependent strength loss due to continuous weathering may bring the slope to failure. Eberhardt et al. (2004) points to the fact that in cases where adversely oriented discontinuities in the slope are highly persistent, failure occurs by propagation of shear plane through only intact rock bridges where kinematic release will require very less internal deformation. This means that deformation in rock mass in such cases is mostly due to weathering, which causes degradation and disintegration due to exposure to adverse climatic conditions. Utilizing the concept of crack propagation in slope highlights another important fact that when discontinuities are critically aligned to the loading direction and stress concentration near the tip of these cracks exceed the strength of the material, fracture propagation will occur in a plane parallel to  $\sigma_1$  (Eberhardt et al. 2004). When a free surface like that of a slope is created,  $\sigma_1$  aligns itself to the topography. The laminations in the rock mass are near parallel to the topography which means crack propagation will be favored in the plane of lamination and brittle failure may contribute as one of the failure mechanism (refer Fig. 5). It is to be noted that majority of these cracks developed following the above argument are tensile in nature, but secondary

**Fig. 8** Comparison of UCS for different laminated rocks with angle of bedding





**Fig. 9** Outcrop of the failed slope showing orthogonal joints, failure direction, and a layer of weathered and nonfissured clay on top

cracks on the other hand may not propagate parallel to  $\sigma_1$ . Bobet and Einstein (1998) argue that secondary cracks initiate in a compressive stress field as shear cracks and often results in spalling of material from the surface. The presence of neighboring cracks significantly influences the development of shear cracks. In a series of multiple cracks which are either coplanar or stepped (joints separated by rock bridge), as in the case of slopes, shear cracks develop in the same plane and links the preexisting cracks directly in the case of coplanar joints and indirectly in the case of stepped cracks. This suggests that in a system of impersistent joint

sets, a complex fracturing system (a combination of tensile and shear cracks) is most likely to develop leading to intense deformation and subsequent failure in rock mass.

The second phase was modeled by applying 40-m head pressure equivalent to around 0.4 MPa from the left boundary of the slope. The hydromechanical simulation was stopped after 30,000 cycles as during this time water was able to migrate until the slope face. The thickness of the aperture was increased and shear strength of joints was reduced to accommodate strength loss due to fluid pressure. At a particular time when fluid reaches the slope face,

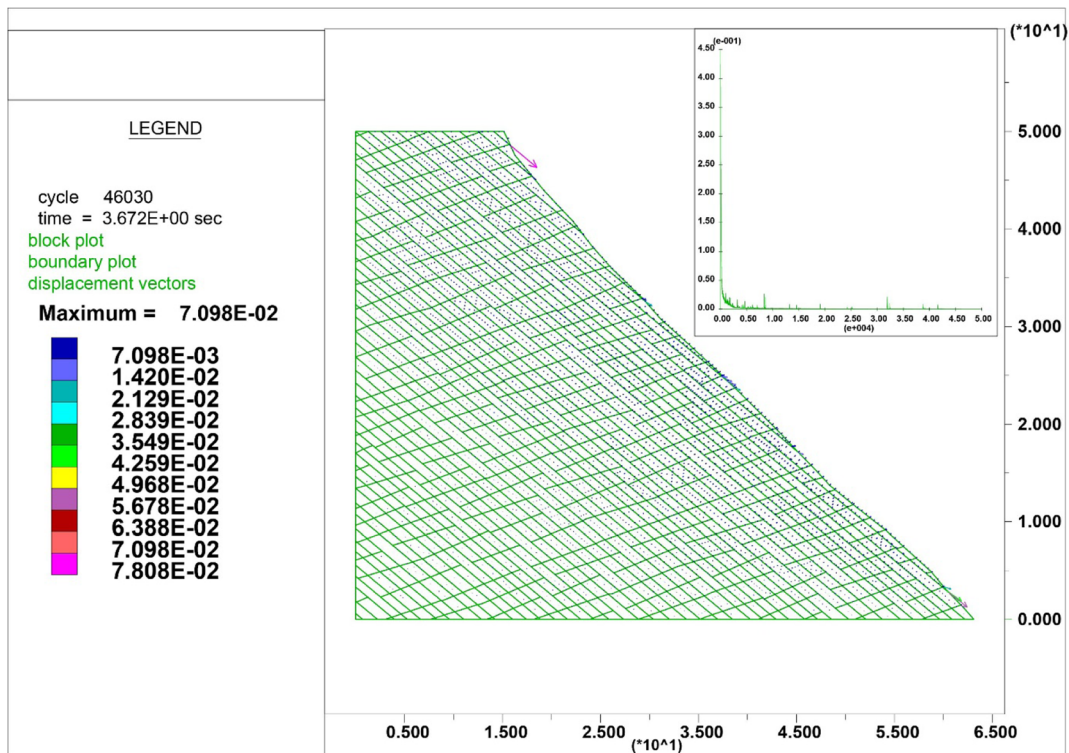


**Fig. 10** Cut slope in equilibrium condition under gravity loading (note: subset indicating zero unbalanced forces at equilibrium)

entire slope face starts showing continuous movement with the maximum displacement observed around 1.2 m near the toe. This increase in hydraulic conductivity and reduction in shear strength exerts tremendous pressure on the blocks enabling complete detachment. Due to the reduction in available shear strength, the movement becomes more pronounced along the daylighting joints, i.e., the lamination planes. The failure plane resembles that of a planar mode as has been observed in the field, also supported by kinematic analysis. The developed failure plane is very shallow, only confined to thickness reaching up to few meters. The most notable result is that the block detachment is seen from the mid portion of the slope which confirms the observation during field investigation where majority of slope mass was seen to be detached from near about similar position (Figs. 9 and 11). Researchers have observed that landslides in weak material like shales/mudstones show characteristic fissuring, dilation, softening, and negative pore pressure and generally fail due to cohesion loss where the shear strength value lies in between peak and residual shear strength (Stead 2016). Although residual shear strength has been largely related to reactivated landslides, several evidence have suggested that residual condition may exist on a part of slip surface even on first-time excavated slopes in clay shales or stiff clays (Mesri and Shahien 2003).

It can be observed from Fig. 12 that the maximum flow rate is  $2.93 \times 10^{-3} \text{ m}^3/\text{s}$  near the left boundary at (A) of the slope, because of point of application of flow pressure. Further, at points B and C, joints are under relatively high confining condition on contrary to the points D and A. Therefore, the inability of the fluid to transmit flow towards the slope face is counteracted by the tightness of joints under confined condition far-off the face. The continued

application of fluid pressure causes water to migrate along available pathways/interconnected fractures toward the slope face. The addition of water creates excess pore pressure within the joints (at point D, Fig. 12) forcing the apertures to open, a process more dominant near slope face with low normal and confining stress (Fig. 12). Opening of joint starts when the equivalent shear strength is just in excess of the initial strength of the joint. These results are quite consistent when compared with the observations made by earlier workers on the experimental study of fluid flow through fractured sample (Walsh 1981; Raven and Gale 1985; Pyrak-Nolte et al. 1988; Pyrak-Nolte and Morris 2000; Singh et al. 2014; Singh et al. 2016a).

A distinct observation made by many researchers confirms that  $Q$  increases with the increase in  $f_p$  and decreases significantly with the increase in applied confining stress. In general, fluid flow through fracture is a function of several parameters such as fluid pressure, fracture aperture, geometry of the fracture, joint wall strength, fracture roughness, confining stress, and more importantly the interconnectivity of the fracture/s (Singh et al. 2015a). An important advantage of this model is that fluid flow is restricted within the rock matrix, and flow occurs through the available pathways/fracture only, which is helpful in simulating the actual conditions present in low porosity rocks, such as mudstone, shale, etc.

#### Remedial measures

The main aim of the implementation of remedial measure is to provide resistance against the movement of most critical failure surface and the zones showing maximum movement. Buttress, piling, rock bolt, retaining structures, and several other techniques are available to attain this task. One of the earliest and most

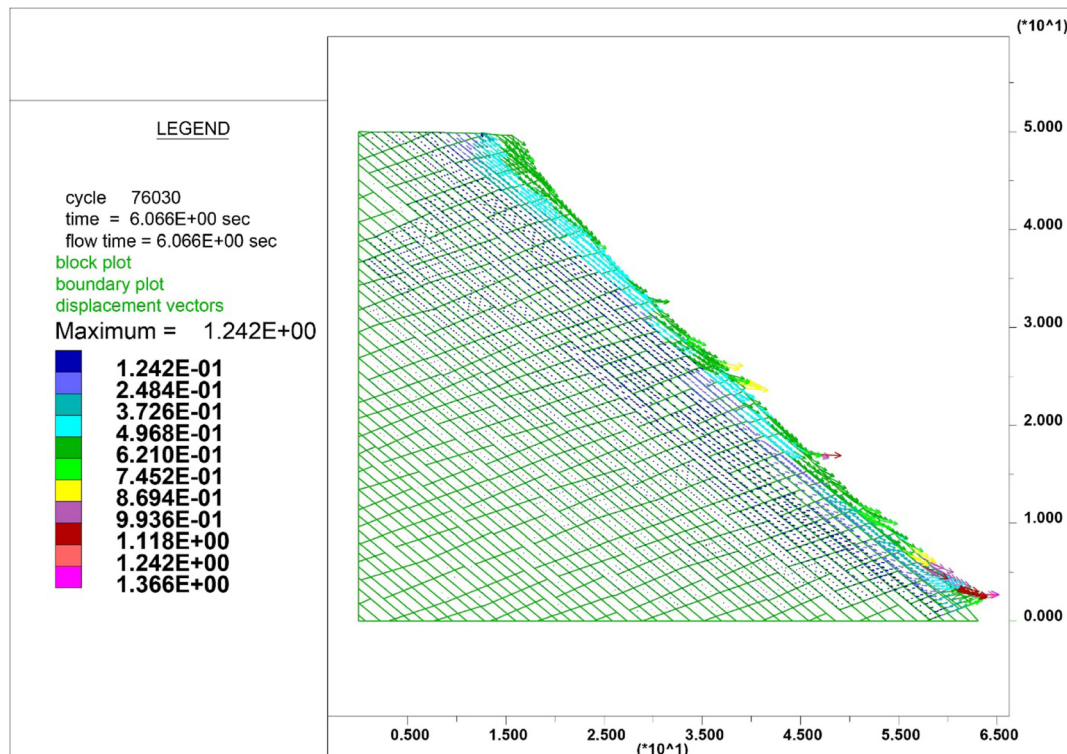


Fig. 11 Displacement vectors in the case of coupled hydromechanical loading condition showing block detachment

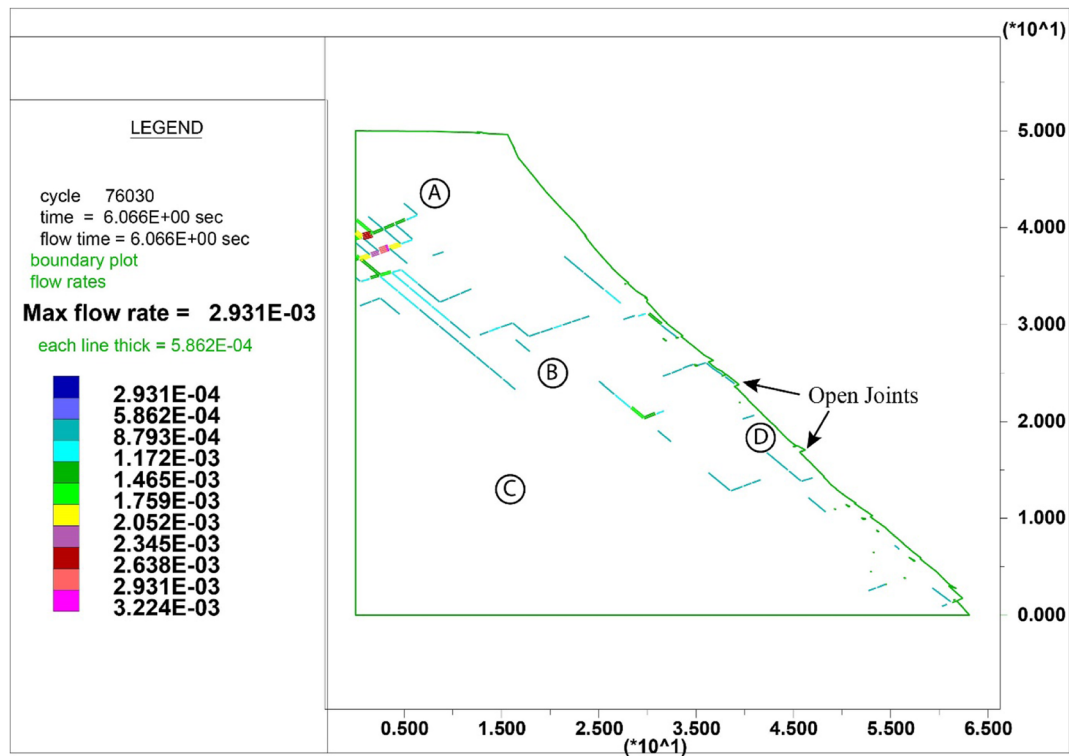


Fig. 12 Flow path and flow rate along the joints leading to block detachment

effective methods used to stabilize the cut slopes have been the retaining structures. In order to effectively design retaining structure, possible modes of failure should be considered. The foundation of structure should be deep enough to prevent base failure. However, it should be noted that still in some cases complete failure of retaining structures has been observed worldwide. The identifiable causes of failure have been excessive seepage and build-up of hydrostatic pressure, overturning of the wall itself and in many cases insufficient foundation depth (Schweizer and Wright 1974). There should be provisions for surface and subsurface drainage including drainage from households to allow water to escape from the slope face and prevent rocks from further weathering. The purpose of horizontal drains would be to decrease the groundwater table in the slide or adjacent areas in order to restrict excess pore pressure build-up. In areas of active slide, surface drainage is a necessary solution to prevent water to percolate and degrade the rocks. When material is excavated along cut slopes, stress release and heaving create additional joints allowing water to percolate deeper causing time-dependent strength reduction eventually leading to slope failure. The rock should be given sufficient time after excavation for stress release and structure should be designed on the basis of residual shear strength value. Concrete lined ditches with proper gradient should be constructed near toe for heavy surface runoff and care must be taken where heaving is possible. Timely checkup should be done to identify the locations to prevent debris to accumulate in the ditches. If possible, additional precaution should be taken to seal the base of the ditches; otherwise, situation may arise where ditches may become a source for water percolation. The maximum allowed load at the crest of the slope should be calculated with a

suitable safety factor value for long-term stability of slope and structure. Additionally, gabion walls may be created by the side of the road for further precaution and strengthening of the toe.

### Conclusion

Problems of slope failure in the exposed weak and jointed stratified rocks are ubiquitous in NE Himalayas, India. Unscientific construction activities aided by heavy precipitation make the problem even more complicated. Therefore, a detailed investigation is made in the failed cut slope of the study area to study the processes and mechanisms that caused slope failure. Investigation involved detailed geomaterial characterization of in situ condition of existing rocks followed by numerical simulation. Numerical simulation is performed under gravity and coupled hydromechanical condition employing distinct element method. The results highlight critical issues in this area, and some of the observations are listed below.

- Settlements are built randomly without prior geological and geotechnical investigations on the exposed weak, stratified, and jointed cut slopes. No proper drainage galleries were observed during field investigation.
- Initial investigation of structural disposition of rock joints and orientation of slope face shows that the bedding parallel joints with a dip amount of  $45^\circ$  daylight on the slope face, an optimum condition for planar mode of failure.
- Anisotropic strength variation is observed when samples are loaded parallel and perpendicular to bedding planes, and the presence of widely spaced orthogonal joints promotes kinematic release of blocks.

- Exposure of rocks to long-term weathering is seen in terms of disintegration and decomposition of surficial material in field. This is further confirmed by the results of slake durability index test which shows significant disintegration and slaking after second cycle. Slaking is attributed to intense weathering in clay-rich rocks leading to breakage of bonds and cementing materials which allow water to ingress deeper causing fragmentation.
- The results of numerical simulation through distinct element method is very interesting and emphasize the process and mechanisms that cause failure in stratified rocks. The slope is stable in the gravity loading condition. Simulation of fluid pressure equivalent to 40-m water head causes joints to open where sufficient confinement is unavailable in addition to reduction of shear strength in joints. Therefore, joints near slope face show maximum opening leading to block detachment from the slope face. The developed failure plane is very shallow and dominantly resembles a planar mode of failure. The maximum displacement is observed near the toe of slope. The maximum flow rate is  $2.93 \times 10^{-3} \text{ m}^3/\text{s}$  near the left boundary. The accumulation of fluid pressure with time forces fluid to migrate along the fractures ultimately leading to slope failure.

### Acknowledgements

This paper is a continuation of the research work published in International Conference on Recent Advances in Rock Engineering (RARE-2016), Bengaluru, India. Authors would like to thank Rock Science and Rock Engineering lab, IIT Bombay and Geological Survey of India, Hyderabad, India, for necessary support and permission to publish this work. Authors are also thankful to the anonymous reviewers and editor for their comments which helped to modify the paper in present form.

### References

ASTM-D4543 (2008) Standard practices for preparing rock Core as cylindrical test specimens and shape tolerances. ASTM:1–9. doi:10.1520/D4543-08

Bell FG, Cripps JC, Culshaw MG (1986) A review of the engineering behaviour of soils and rocks with respect to groundwater. *Geol Soc London Eng Geol Spec Publ* 3:1–23. doi:10.1144/GSL.ENG.1986.003.01.01

Bjerrum L (1967) Progressive failure in slopes of overconsolidated plastic clay and clay shales. *J Soil Mech Found Div* 93:1–49

Bobet A, Einstein HH (1998) Fracture coalescence in rock-type materials under uniaxial and biaxial compression. *Int J Rock Mech Min Sci* 35:863–888. doi:10.1016/S0148-9062(98)00005-9

Bobet A, Fakhimi A, Johnson S et al (2009) Numerical models in discontinuous media: review of advances for rock mechanics applications. *J Geotech Geoenviron* 135:1547–1561. doi:10.1061/(ASCE)GT.1943-5606.0000133

Bovis MJ (1985) Earthflows in the interior plateau, Southwest British Columbia. *Can Geotech J* 22:313–334. doi:10.1139/t85-045

Brace WF (1978) A note on permeability changes in geologic material due to stress. *Pure Appl Geophys PAGEOPH* 116:627–633. doi:10.1007/BF00876529

Chen C-S, Pan E, Amadei B (1998) Determination of deformability and tensile strength of anisotropic rock using Brazilian tests. *Int J Rock Mech Min Sci* 35:43–61. doi:10.1016/S0148-9062(97)00329-X

Cundall PA, Hart RD (1992) Numerical Modelling of Discontinua. *Eng Comput* 9:101–113. doi:10.1108/eb023851

Donath F (1961) Experimental study of shear failure in anisotropic rocks. *Geol Soc Am Bull* 72:985–990

Eberhardt E, Stead D, Coggan JS (2004) Numerical analysis of initiation and progressive failure in natural rock slopes—the 1991 Randa rockslide. *Int J Rock Mech Min Sci* 41:69–87. doi:10.1016/S1365-1609(03)00076-5

Eberhardt E, Stead D, Stimpson B, Read RS (1998) Identifying crack initiation and propagation thresholds in brittle rock. *Can Geotech J* 35:222–233

Einstein H, Veneziano D, Baecher GB, O'Reilly K (1983) The effect of discontinuity persistence on rock slope stability. *Int J Rock Mech Min Sci Geomech Abstr* 20:227–236

Evans SG, Hungr O (1993) The assessment of rockfall hazard at the base of talus slopes. *Can Geotech J* 30:620–636. doi:10.1139/t93-054

Gao Q, Tao J, Hu J, Yu XB (2015) Laboratory study on the mechanical behaviors of an anisotropic shale rock. *J Rock Mech Geotech Eng* 7:213–219. doi:10.1016/j.jrmge.2015.03.003

Geertsema M, Cruden DM (2009) Rock movements in northeastern British Columbia. *Proceedings of landslide processes conference*. pp 31–36

Genger M (1985) Progressive failure in stratified and jointed rock mass. *Rock Mech Rock Eng* 18:267–292

Ghosh S, Chakchhuak L (2013) Landslip kills 10 in Aizawl. *The Telegraph*

Gökçeoglu C, Ulusay R, Sönmez H (2000) Factors affecting the durability of selected weak and clay-bearing rocks from Turkey, with particular emphasis on the influence of the number of drying and wetting cycles. *Eng Geol* 57:215–237. doi:10.1016/S0013-7952(00)00031-4

Goodman RE (2013) Toppling - A fundamental failure mode in discontinuous materials-description and analysis. *Geo-Congress 2013* © ASCE 2013. pp 2348–2378

Indraratna B, Ranjith PG, Gale W (1999) Single phase water flow through rock fractures. *Geotech Geol Eng* 17:211–240

Jing L, Hudson JA (2002) Numerical methods in rock mechanics. *Int J Rock Mech Min Sci* 39:409–427. doi:10.1016/S1365-1609(02)00065-5

Jing L, Ma Y, Fang Z (2001) Modeling of fluid flow and solid deformation for fractured rocks with discontinuous deformation analysis (DDA) method. *Int J Rock Mech Min Sci* 38:343–355. doi:10.1016/S1365-1609(01)00005-3

Kainthola A, Singh PK, Singh TN (2015) Stability investigation of road cut slope in basaltic rockmass, Mahabaleshwar, India. *Geosci Front* 6:837–845. doi:10.1016/j.gsf.2014.03.002

Kainthola A, Singh PK, Wasknik AB, Singh TN (2012) Distinct element Modelling of Mahabaleshwar road Cut Hill slope. *Geomaterials* 2:105–113. doi:10.4236/gm.2012.24015

Khanlari G, Rafiei B, Abdilor Y (2015) Evaluation of strength anisotropy and failure modes of laminated sandstones. *Arab J Geosci* 8:3089–3102. doi:10.1007/s12517-014-1411-1

Lee DH, Yang YE, Lin HM (2007) Assessing slope protection methods for weak rock slopes in southwestern Taiwan. *Eng Geol* 91:100–116. doi:10.1016/j.enggeo.2006.12.005

Lisjak A, Grasselli G (2014) A review of discrete modeling techniques for fracturing processes in discontinuous rock masses. *J Rock Mech Geotech Eng* 6:301–314. doi:10.1016/j.jrmge.2013.12.007

Mahanta B, Singh HO, Singh PK, Kainthola A, Singh TN (2016) Stability analysis of potential failure zones along NH-305. India. *Nat Hazards* 83:1341–1357. doi:10.1007/s11069-016-2396-8

Martin CD, Giger S, Lanyon GW (2016) Behaviour of weak shales in underground environments. *Rock Mech Rock Eng* 49:673–687. doi:10.1007/s00603-015-0860-5

Mesri G, Shahien M (2003) Residual shear strength mobilized in first-time slope failures. *J Geotech Geoenvironmental Eng* 129:12–31. doi:10.1061/(ASCE)1090-0241(2003)129:112

Miščević P, Vlastelica G (2014) Impact of weathering on slope stability in soft rock mass. *J Rock Mech Geotech Eng* 6:240–250. doi:10.1016/j.jrmge.2014.03.006

Nasser MHB, Rao KS, Ramamurthy T (2003) Anisotropic strength and deformation behavior of Himalayan schists. *Int J Rock Mech Min Sci* 40:3–23. doi:10.1016/S1365-1609(02)00103-X

Picarelli L, Urciuoli G, Mandolini A, Ramondini M (2006) Softening and instability of natural slopes in highly fissured plastic clay shales. *Nat Hazards Earth Syst Sci* 6:529–539. doi:10.5194/nhess-6-529-2006

Pyrak-Nolte LJ, Cook NGW, Nolte DD (1988) Fluid percolation through single fractures. *Geophys Res Lett* 15:1247–1250

Pyrak-Nolte LJ, Morris JP (2000) Single fractures under normal stress: the relation between fracture specific stiffness and fluid flow. *Int J Rock Mech Min Sci* 37:245–262. doi:10.1016/S1365-1609(99)00104-5

- Raven KG, Gale JE (1985) Water flow in a natural rock fracture as a function of stress and sample size. *Int J Rock Mech Min Sci Geomech Abstr* 22:251–261. doi:10.1016/0148-9062(85)92952-3
- Regmi AD, Yoshida K, Dhital MR, Devkota K (2013) Effect of rock weathering, clay mineralogy, and geological structures in the formation of large landslide, a case study from Dumre Besi landslide, lesser Himalaya Nepal. *Landslides* 10:1–13. doi:10.1007/s10346-011-0311-7
- Schweizer RJ, Wright SG (1974) A survey and evaluation of remedial measures for earth slope stabilization. doi: Research Report 161-2F
- Singh KK, Singh DN, Gamage RP (2016a) Effect of sample size on the fluid flow through a single fractured granitoid. *J Rock Mech Geotech Eng* 8:329–340. doi:10.1016/j.jrmge.2015.12.004
- Singh KK, Singh DN, Ranjith PG (2015a) Laboratory simulation of flow through single fractured granite. *Rock Mech Rock Eng* 48:987–1000. doi:10.1007/s00603-014-0630-9
- Singh KK, Singh DN, Ranjith PG (2014) Simulating flow through fractures in a rock mass using analog material. *Int J Geomech* 14:8–19. doi:10.1061/(ASCE)GM.1943-5622.0000295
- Singh PK, Das R, Singh KK, Singh TN (2016b) Landslide in fractured and stratified rocks- a case from Aizawl, Mizoram, India. In: Venkatesh H, Venkateswarlu V (eds) International conference on recent advances in rock engineering (RARE-2016). Atlantis Press, Bengaluru, pp. 189–194
- Singh PK, Kainthola A, Panthee S, Singh TN (2016c) Rockfall analysis along transportation corridors in high hill slopes. *Environ Earth Sci*. doi:10.1007/s12665-016-5489-5
- Singh PK, Kainthola A, Prasad S, Singh TN (2015b) Protection measures on the failed cut-slope along the free expressway, Chembur, Mumbai, India. *J Geol Soc India* 86:687–695
- Singh PK, Tripathy A, Kainthola A, Mahanta B, Singh V, Singh TN (2016d) Indirect estimation of compressive and shear strength from simple index tests. *Eng Comput*. doi: 10.1007/s00366-016-0451-4
- Stead D (2016) The influence of shales on slope instability. *Rock Mech Rock Eng* 49:635–651. doi:10.1007/s00603-015-0865-0
- Števančić D, Mišćević P (2007) The durability characterization of selected marls from Dalmatian region in Croatia. XVIII European Young Geotechnical Engineers' Conference
- Tang H, Yong R, Ez Eldin MAM (2016) Stability analysis of stratified rock slopes with spatially variable strength parameters: the case of Qianjiangping landslide. *Bull Eng Geol Environ*. doi:10.1007/s10064-016-0876-4
- Urciuoli G (1990) Contributo alla caratterizzazione geotecnica delle frane dell'Appennino, Quaderni dell'Istituto di Tecnica delle Fondazioni e Costruzioni in Terra, Università di Napoli Federico II, n. 1
- Walsh JB (1981) Effect of pore pressure and confining pressure on fracture permeability. *Int J Rock Mech Min Sci Geomech Abstr* 18:429–435. doi:10.1016/0148-9062(81)90006-1
- Witherspoon PA, Wang JSY, Iwai K, Gale JE (1980) Validity of cubic law for fluid flow in a deformable rock fracture. *Water Resour Res* 16:1016–1024. doi:10.1029/WR016i006p01016
- Wong LNY, Einstein HH (2009) Crack coalescence in molded gypsum and Carrara marble: part 1. Macroscopic observations and interpretation. *Rock Mech Rock Eng* 42:475–511. doi:10.1007/s00603-008-0002-4
- Yagiz S (2001) Overview of classification and engineering properties of shales for design considerations. *Constr Mater Issues*:156–165
- Yaşar E (2001) Failure and failure theories for anisotropic rocks. 17th International Mining Congress and Exhibition of Turkey-IMCET 2001. Turkey, pp 417–424

---

**P. K. Singh · T. N. Singh**

Department of Earth Sciences,  
Indian Institute of Technology Bombay,  
Mumbai-400076, India

**K. K. Singh** (✉)

Geohazards and Engineering Geology Division,  
Geological Survey of India,  
Bandlaguda, Hyderabad, 500068, India  
e-mail: karfuekunal@gmail.com